

FINITE ELEMENT MODELLING OF SHEARED FLOW EFFECTS ON THE RADIATION CHARACTERISTICS OF ACOUSTIC SOURCES IN A CIRCULAR DUCT

JAMES E. STECK

Mechanical Engineering, The Wichita State University, Wichita, KS 67208, U.S.A.

AND

WALTER EVERSMAN

Mechanical and Aerospace Engineering, Engineering Mechanics, University of Missouri, Rolla, MO 65401, U.S.A.

SUMMARY

The recent interest in propeller noise generation, stimulated by development of new propeller types for commercial propjets, has generated a need for the ability to measure the noise characteristics of propellers. However, wind tunnel noise measurements are affected by reflections from the wind tunnel walls. Computer codes predicting the free-field noise of a propeller and its noise field in a circular wind tunnel allow validating the use of wind tunnel measurements to predict free-field noise characteristics. A wind tunnel contains flow which is uniform in the duct axial direction, but can vary in the radial direction. It can be shown that a third-order differential equation governs the acoustic pressure field for such a duct containing radially sheared subsonic flow. This third-order problem is then posed as a coupled pair of equations which are second-order in terms of acoustic density and first-order in terms of an artificial variable which represents the effects of the flow being sheared. It is shown that this form of the problem allows a natural extension of the existing numerical solution techniques for non-sheared flow. The sheared flow problem is presented, and a finite element method is developed to yield a solution for propeller-type acoustic forces. The finite element code and method are refined with numerical experiments, and results are presented for a specific propeller and duct geometry. Good agreement is shown between this method and an alternate approach to the sheared flow problem using a piecewise constant representation of the velocity in the boundary layer. This validates both the numerical methods.

KEY WORDS Finite elements Aeroacoustics Propellers Sheared flow

INTRODUCTION

The acoustic radiation characteristics of a circular duct are of interest from the standpoint of assessing the effect a wind tunnel wall has on acoustic testing of propellers. Acoustic noise measurements of propellers are generally made in wind tunnels under simulated flight conditions. These measurements can be greatly affected by the presence of the tunnels walls, which reflect some of the incident sound. They also change the nature of the flow around the propeller from that of actual flight conditions by causing the velocity profile to be sheared, rather than be uniform. A circular duct, containing propeller-type acoustic sources and a *uniform velocity profile*, has been successfully modelled by Eversman and Baumeister¹ and Eversman² using a finite element method to solve the governing second-order convected wave equation. That method

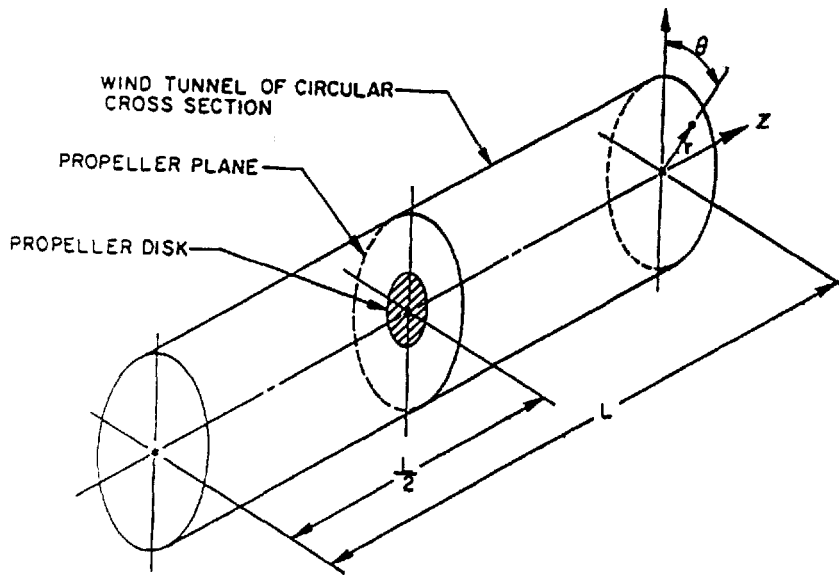


Figure 1. The circular duct domain with a cylindrical co-ordinate system

initially modelled a duct with a hard wall¹ and, subsequently, a duct with an absorbing lining.³ When a sheared velocity profile is included, the governing wave equation becomes a third-order partial differential equation. A mixed finite element method is presented here which solves this wave equation for sheared flow by addressing it as a coupled pair of differential equations, one second-order, the other a first-order equation.

Acoustic waves in air are considered to be of small density, and velocity perturbations on a known mean flow field. The duct is assumed to have a circular cross-section which is uniform in the axial direction. It contains a mean air flow which varies only in the radial direction and has no swirl. A representative duct fluid domain is shown in Figure 1. The problem is described by the usual compressible-fluids equations: conservation of mass, equation of state, conservation of momentum and a Stokes' law relationship. These equations can be combined and linearized to yield a third-order wave equation in terms of acoustic density alone. This has been amply demonstrated by Mohring in Reference 4. Thus, given the Mach number profile and the acoustic body force vector \mathbf{f} ; the acoustic density ρ is to be found as a function of time and cylindrical space-coordinates, such that

$$\frac{D}{Dt} \left[\frac{D^2 \rho}{Dt} - \nabla^2 \rho + \nabla \cdot \mathbf{f} \right] + 2 \frac{\partial M}{\partial r} \frac{\partial^2 \rho}{\partial x \partial r} = 0 \quad (1)$$

and such that a boundary condition in terms of the acoustic admittance of the duct lining holds at the duct wall, and where

$$\frac{D}{Dt} = \left(\frac{\partial}{\partial t} - M \frac{\partial}{\partial x} \right).$$

The acoustic sources are assumed to be periodic in the time co-ordinate and in the cylindrical co-ordinate, θ , as is the case for propellers. Using a Gutin-type model, the propeller source functions and the acoustic density can be represented as Fourier series.^{5,6} Since this propeller

model is represented in the frequency domain, the governing equations are transformed to the frequency domain. Taking Fourier transforms with respect to time and the co-ordinate θ gives the problem: given a Mach number profile M as a function of the axial co-ordinate, and an acoustic body force vector function $\{f_i\}$, having the Fourier transform $\{\hat{f}_i^{nm}\}$, for each integer n, m find $\hat{\rho}$ such that

$$\left(i\hat{k}_n + M \frac{\partial}{\partial x_2}\right) \left[\left(i\hat{k}_n + M \frac{\partial}{\partial x_2}\right)^2 \hat{\rho} - \frac{\partial^2}{\partial x_1^2} \hat{\rho} - \frac{1}{x_1} \frac{\partial}{\partial x_1} \hat{\rho} + \frac{m^2}{x_1^2} \hat{\rho} - \frac{\partial^2}{\partial x_2^2} \hat{\rho} + \frac{\partial}{\partial x_1} \hat{f}_1^{nm} + \frac{im}{x_1} \hat{f}_2^{nm} + \frac{1}{x_1} \hat{f}_3^{nm} + \frac{\partial}{\partial x_2} \hat{f}_3^{nm} \right] + 2 \frac{\partial M}{\partial x_1} \left[\frac{\partial^2}{\partial x_1 \partial x_2} \hat{\rho} - \frac{\partial}{\partial x_2} \hat{f}_1^{nm} \right] = 0 \quad (2)$$

and such that

$$\frac{\partial}{\partial x_1} \hat{\rho} = -i\hat{k}_n \left(1 - \frac{iM}{\hat{k}_n} \frac{\partial}{\partial x_2}\right)^2 \bar{A} \hat{\rho} \quad (\text{at } x_1 = 1), \quad (3)$$

where we have defined

$$\hat{k}_n = \omega_n \frac{R}{\bar{c}} \quad \text{and} \quad \omega_n = \frac{2\pi n}{T}$$

and where T is the fundamental period of the source functions. Also the radial spatial co-ordinate r and the axial spatial co-ordinate z have been non-dimensionalized by the duct radius R to yield the co-ordinates x_1 in the radial direction and x_2 in the axial direction; the acoustic density and source terms have been non-dimensionalized by the mean acoustic density $\bar{\rho}$, the duct radius R , and the mean speed of sound \bar{c} .

For uniform flow, $\partial M / \partial x_1 = 0$, and the governing differential equation is the second-order equation enclosed by the first set of brackets of equation (2). This problem has been successfully solved by Eversman and Baumeinter¹ using a finite element method. This finite element method, developed by Eversman for uniform flow, is used here as a basis upon which a finite element method is constructed to solve the sheared flow problem. Toward this end, the third-order differential equation (2) is written as two coupled equations: one second-order in terms of acoustic density and one first-order in terms of a new variable 'd', which is defined to be equal to the second-order terms inside the first set of brackets of equation (2). The problem obtained is: find $\hat{\rho}$ and d such that

$$\left(i\hat{k}_n + M \frac{\partial}{\partial x_2}\right) d + 2 \frac{\partial M}{\partial x_1} \left[\frac{\partial^2}{\partial x_1 \partial x_2} \hat{\rho} + \frac{\partial}{\partial x_2} \hat{f}_1^{nm} \right] = 0 \quad (4)$$

and

$$\left(i\hat{k}_n + M \frac{\partial}{\partial x_2}\right)^2 \hat{\rho} - \frac{\partial^2}{\partial x_1^2} \hat{\rho} - \frac{1}{x_1} \frac{\partial}{\partial x_1} \hat{\rho} + \frac{m^2}{x_1^2} \hat{\rho} - \frac{\partial^2}{\partial x_2^2} \hat{\rho} + \frac{\partial}{\partial x_1} \hat{f}_1^{nm} + \frac{im}{x_1} \hat{f}_2^{nm} + \frac{1}{x_1} \hat{f}_3^{nm} + \frac{\partial}{\partial x_2} \hat{f}_3^{nm} = d \quad (5)$$

and such that

$$\frac{\partial}{\partial x_1} \hat{\rho} = -i\hat{k}_n \left(1 - \frac{iM}{\hat{k}_n} \frac{\partial}{\partial x_2}\right)^2 \bar{A} \hat{\rho} \quad (\text{at } x_1 = 1).$$

The new variable, d , represents the effects of the shear layer since $d=0$ when the Mach number, M , is constant.

A FINITE ELEMENT METHOD

A finite element method^{7,8} is developed which solves the problem of equations (4) and (5) for an arbitrary acoustic source distribution in a duct with hard walls. For a hard-walled duct, the acoustic admittance \bar{A} is zero,^{9,10} simplifying the boundary condition at the wall. For a soft-walled duct, the boundary term in the above equation is implemented in the finite element formulation, but for the purposes of clarity, only a hard-walled duct is considered in the remainder of this paper. Following the work of Eversman and Baumeister¹ for the second-order equation, the infinite circular duct domain is truncated at $x_2 = \pm L$, giving the finite domain $\bar{\Omega}_{1,2}$ of Figure 2. The acoustic sources are assumed to be zero everywhere except in a region 'near' the axis $x_2 = 0$. Then as L becomes large, the solution to the forced problem at the ends of the duct ($x_2 = \pm L$) approaches a solution to the homogeneous or unforced problem. This gives a boundary condition to be imposed on the finite domain at $x_2 = \pm L$. The solution of the forced problem must match the form of the general homogeneous (eigenvalue) solution to the unforced problem at the ends of the duct.¹¹ A specific homogeneous solution is specified by the selection of values for the constants a_l and b_l in the expressions

$$\rho_h(x_1, x_2) = \sum_{\text{all } l} a_l P_l(x_1) e^{-iK_l \hat{k}_n x_2},$$

$$d_h(x_1, x_2) = \sum_{\text{all } l} b_l D_l(x_1) e^{-iK_l \hat{k}_n x_2},$$
(6)

where K_l are the eigenvalues of the unforced problem, and P_l and D_l are the eigenfunctions. Posing the problem now in the L_2 integral, or weakened sense, integrating by parts and applying the boundary conditions gives the following problem in terms of integral operators ϕ and b . Let

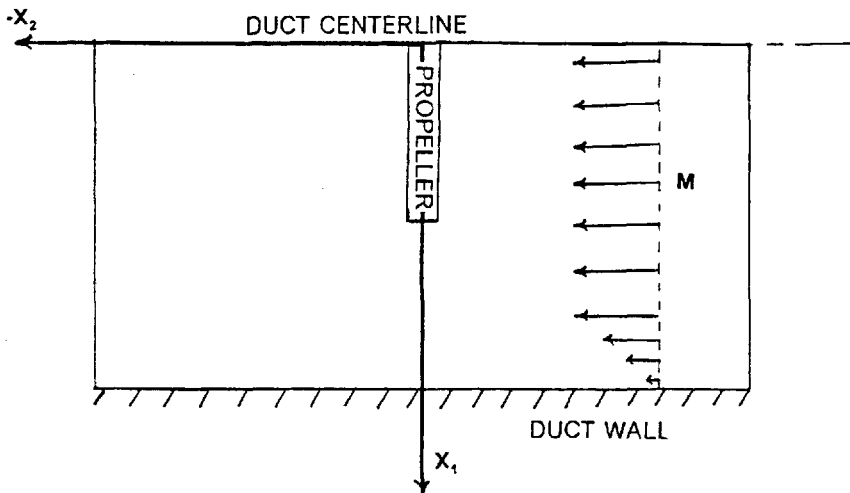


Figure 2. The finite problem domain after Fourier decomposition, showing a sheared flow in one-fifth of the duct near the wall

ϕ and b be defined as

$$\begin{aligned} \phi[(\rho, A^+, A^-, d), (h, S^+, S^-, g)] &= \phi(\tilde{\rho}, \tilde{h}) \\ &= \int_{\bar{\Omega}_{1,2}} \left[\left(\frac{m^2}{x_1^2} - k_n^2 \right) \rho h + \frac{\partial \rho}{\partial x_1} \frac{\partial h}{\partial x_1} - \frac{1}{x_1} \frac{\partial \rho}{\partial x_1} h + (1 - M^2) \frac{\partial \rho}{\partial x_2} \frac{\partial h}{\partial x_2} \right. \\ &\quad \left. + ik_n M \left(\frac{\partial \rho}{\partial x_2} h - \rho \frac{\partial h}{\partial x_2} \right) - dh \right] x_1 dx_1 dx_2 \\ &\quad + \int_{\bar{\Omega}_{1,2}} \left[d \left(ik_n - M \frac{\partial}{\partial x_2} \right) g - 2 \frac{\partial M}{\partial x_1} \frac{\partial \rho}{\partial x_1} \frac{\partial g}{\partial x_2} \right] x_1 dx_1 dx_2 \\ &\quad + \int_0^1 \left[(\rho - A_2^\pm) S_2^\pm \right]_{x_2 = \pm L} x_1 dx_1 + \int_0^1 \pm [h ik_n (MA_2^\pm - (M^2 - 1)A_3^\pm) \\ &\quad + 2 \frac{\partial M}{\partial x_1} \frac{\partial A_2^\pm}{\partial x_1} g + MA_1^\pm g]_{x_2 = \pm L} x_1 dx_1 \end{aligned} \quad (7)$$

$$b((h, S^+, S^-, g)) = b(\tilde{h}) = \int_{\bar{\Omega}_{1,2}} \left\{ 2 \frac{\partial M}{\partial x_1} \frac{\partial f_1}{\partial x_2} g - \left[\frac{1}{x_1} f_1^{nm} + \frac{im}{x_1} f_2^{nm} + \frac{\partial f_1^{nm}}{\partial x_1} + \frac{\partial f_3^{nm}}{\partial x_2} \right] h \right\} x_1 dx_1 dx_2. \quad (8)$$

We have the following *weak problem*: given Mach number M as a function of x_1 and $\{f_i^{nm}\}$ as Fourier coefficients of $\{f_i\}$, for each n, m , find $\tilde{\rho} = (\rho, A^+, A^-, d) \in P \times E^+ \times E^- \times D$ such that

$$\phi(\tilde{\rho}, \tilde{h}) = b(\tilde{h}) \quad (9)$$

for all weight functions $\tilde{h} = (h, S^+, S^-, g) \in H \times E^+ \times E^- \times G$ where E^+ and E^- are function spaces containing all solutions to the unforced homogeneous (eigenvalue) problem at respective ends of the duct, P and H are function spaces which are collections of all functions on the domain $\bar{\Omega}_{1,2}$ with integrable derivatives, D and G are collections of all functions on $\bar{\Omega}_{1,2}$ which are integrable and have integrable first-order derivatives with respect to x_2 . This problem is now a *weaker* formulation of the original problem, as only one derivative of the acoustic density ρ is required to exist and be integrable.

The problem of equation (9) is solved using a finite element technique^{7,8,12} which involves constructing approximations to the solution spaces and weight function spaces of problem (9). These spaces are constructed by dividing the problem domain into a finite number of subdomains, or elements. Then, on each element, a typical function belonging to the space is approximated by a polynomial curve fit. The functions spaces associated with the boundary conditions at the ends of the duct are approximated by using a finite number of the terms in the sum representing the homogeneous solution. If P_h , D_h , H_h , and G_h are function spaces (sets containing functions) which are finite element approximations (polynomials on each element) to the functions in the exact spaces P , D , H , and G , then an approximate problem can be written as equation (9) with the exact solution and weight spaces replaced by the approximate spaces.

For each n, m , find a solution ρ belonging to the set P_h of continuous functions approximated on an element by a *biquadratic* polynomial, and find d belonging to the set D_h of functions approximated on an element by a *bilinear* polynomial and continuous in the x_2 direction, and A^+ and A^- as truncated homogeneous solutions at each end of the duct such that

$$\phi[(\rho, A^+, A^-, d), (h, S^+, S^-, g)] = b[(h, S^+, S^-, g)] \quad (10)$$

for all arbitrary weight functions h belonging to the set H_h of continuous functions approximated on an element by a *biquadratic* polynomial, and all g belonging to the set G_h of functions approximated on an element by a *bilinear* polynomial and continuous in the x_2 direction, and S^+ and S^- as arbitrary truncated homogeneous solutions at each end of the duct.

The number and size of the elements, as well as the choice of quadratic elements for the functions ρ and h are based on the work of Eversman and Baumeister in solving the second-order equation governing non-sheared flow.¹ This work has shown that biquadratic approximations for acoustic density are necessary to achieve an accurate representation for acoustics problems with a manageable number of degrees of freedom. The initial use of bilinear elements for the function d is suggested by the form of equation (7). The first set of brackets in this equation contains terms essentially requiring d to be equal to derivatives of ρ up to first order. Thus, if ρ is approximated by a quadratic function, its first derivatives are approximated by linear functions, thus suggesting that only a linear approximation might be needed for the function d . The second set of brackets in equation (7), however, contains terms, which by the same rationalization suggest that d be linear in the x_1 direction and, perhaps quadratic in the x_2 direction; yet, this analysis is complicated by the fact that the weight function g will be approximated with the same approximation chosen for the function d . This suggests performing some numerical experiments to investigate appropriate orders of approximations for the solution functions and weight functions.

REFINING THE FINITE ELEMENT SOLUTION

To facilitate the investigation of some numerical aspects of the approximate forced problem, some nomenclature is needed concerning the eigenvalues in the representation of the general solution to the unforced problem for an unlined hard-walled duct. Eigenvalues with non-zero imaginary parts are related to what are called cut-off eigenmodes, since the amplitude of the homogeneous solution corresponding to a cut-off eigenmode decays as the mode propagates in the duct axial direction, x_2 . Terms corresponding to eigenvalues having zero imaginary parts are related to what are called cut-on eigenmodes, since the amplitude of the homogeneous solution does not decay appreciably as a function of the axial direction.

Now the forced problem is addressed. To validate the computer code and to investigate the validity of the numerical technique, the results of some check cases are presented. Consider again the duct domain and the attached co-ordinate system shown in Figure 2. A cut-on mode, which propagates downstream, is launched into the upstream end of the duct. This is accomplished via the boundary condition at this end by requiring the solution at the end to match the form of the general homogeneous solution at that end, plus a term for the launched mode. The acoustic forcing terms are set to zero. The finite element problem is formed and solved using a standard 'frontal' solution technique.¹² A solution of problem (10) is shown as a contour plot of acoustic density in Figure 3 and as a 3D plot of acoustic density plotted in the vertical direction as a function of position in the duct, (x_1, x_2) , in Figure 4. The centreline of the duct, and the duct wall, are shown on the plots to orient the position of the duct with respect to the axis system shown.

Figures 3 and 4 are the results of launching a cut-on mode into one end of the duct. Since the mode is cut-on, it should propagate through the duct without decay, maintaining its shape throughout the length of the duct. This indeed is the case, as evidenced by the constant shape in Figure 4 and the straight constant pressure lines in the pressure contour plot. Figure 5 contains a 3D plot of the function d plotted vertically on the duct domain for this launched cut-on mode. Next, a mode that is cut-off is launched into the duct, resulting in Figure 6, which represents 3D plots of acoustic density and the function d , respectively. A cut-off mode should maintain a constant shape but should decay in magnitude as it travels down the duct. This again is the case

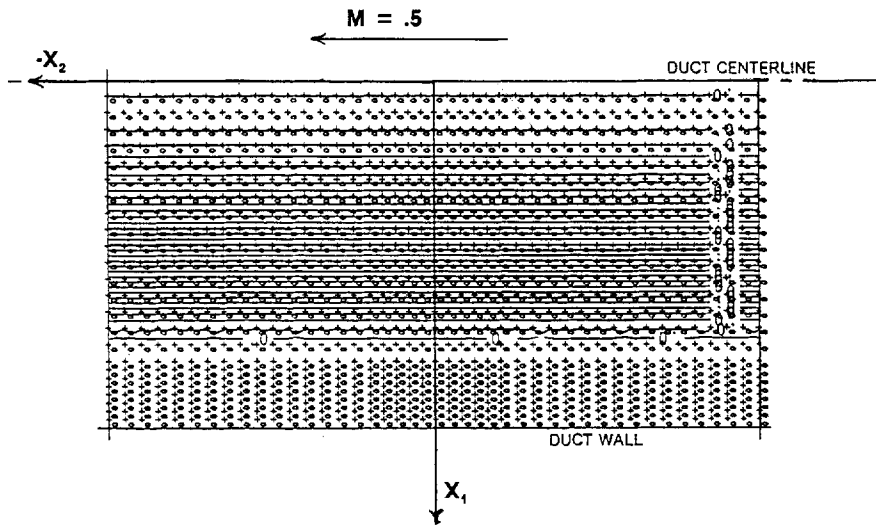


Figure 3. Acoustic density amplitude lines for a cut-on mode launched into the upstream end of the duct, with sheared flow near the wall

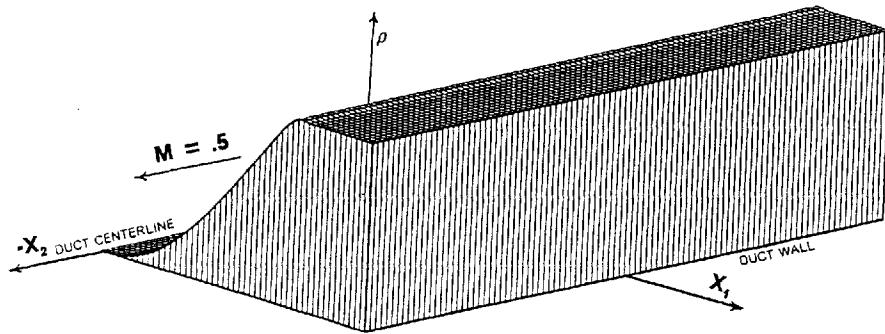


Figure 4. Acoustic density amplitude as a function of position in the duct for a cut-on mode launched into the upstream end of the duct, with sheared flow near the wall

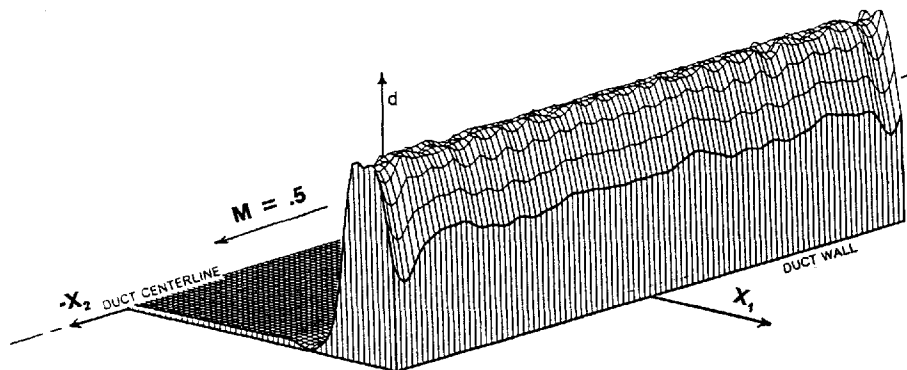


Figure 5. Amplitude of the function d as a function of position in the duct for a cut-on mode launched into the upstream end of the duct, with sheared flow near the wall

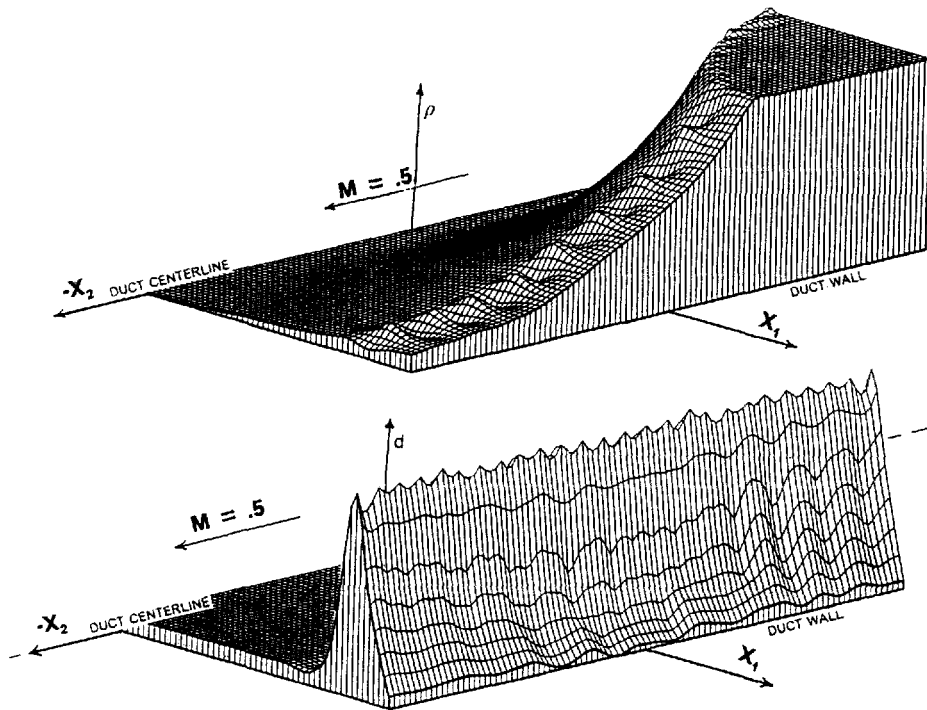


Figure 6. Acoustic density amplitude and amplitude of the function d as a function of position in the duct, for a cut-off mode launched into the upstream end of the duct, with sheared flow near the wall, using four elements across the region of sheared flow, and bilinear approximation for d

as evidenced by the figures, however, the periodic oscillation appearing as bumps on the pressure plot suggests that numerical errors might be present in the solution. Also the plot of the function d shows that it does not decay down the duct, as one might expect.

Figures 3–6 were calculated using a finite element mesh having 21 elements in the axial direction and 12 elements in the radial direction, with four elements across the boundary layer. Figure 7 shows the effect of refining the mesh to a 21×18 grid with eight elements across the boundary layer. The pressure plot is now smooth, and the plot of the function d shows decay axially but indicates numerical error. This improvement with mesh refinement suggests that d is not being approximated accurately enough for the problem as posed in equation (10). To improve the accuracy of the function d , the finite element *bilinear* polynomial approximation of d is replaced by a more accurate *biquadratic* polynomial approximation. Thus, the refined mesh case (21×18) is run using biquadratic quadrilateral elements for both acoustic density and the function d , resulting in Figure 8. Although these results look better, the need for the high-order approximation of the function d is somewhat perplexing, especially in light of the large numerical error evidenced in the 3D plot of d , Figure 7, for a linear approximation.

Let us examine the weak problem of equation (9) as applied to the mode-launching check cases. The acoustic forcing terms are zero. Since the weak problem must hold for any h and g in the specified weight function spaces, choose $g=0$ and h to be a function which is zero on the

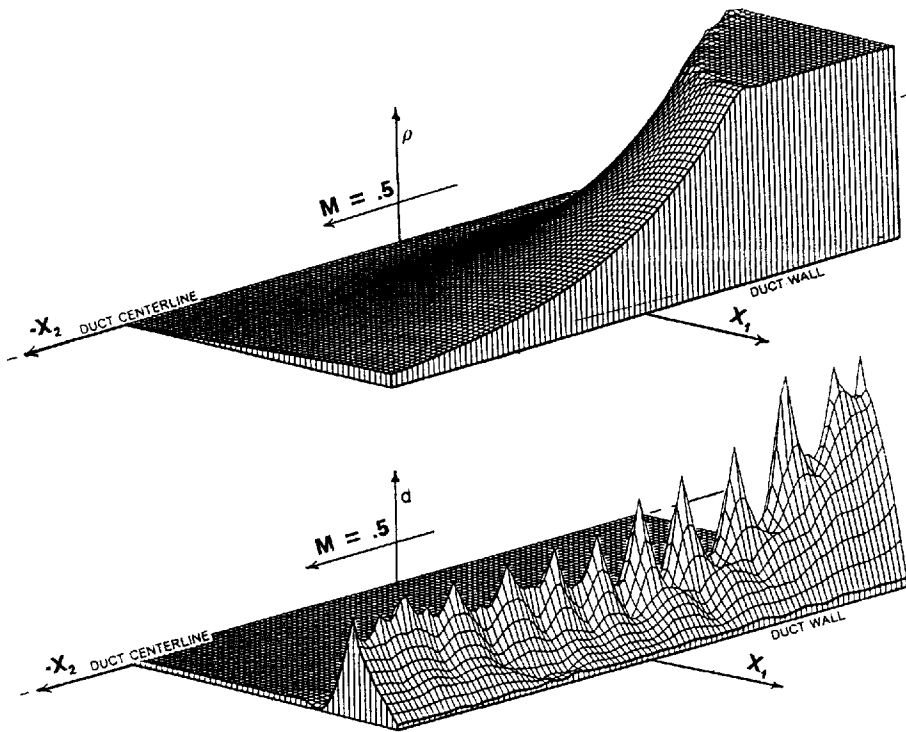


Figure 7. Same case as Figure 6, with eight elements across the region of sheared flow and a bilinear approximation for d

boundary and non-zero over some interior region Ω_{int} . Then equation (9) becomes

$$\int_{\Omega_{int}} \left[\left(\frac{m^2}{x_1^2} - k_n^2 \right) \rho h + \frac{\partial \rho}{\partial x_1} \frac{\partial h}{\partial x_1} - \frac{1}{x_1} \frac{\partial \rho}{\partial x_1} h + (1 - M^2) \frac{\partial \rho}{\partial x_2} \frac{\partial h}{\partial x_2} + ik_n M \left(\frac{\partial \rho}{\partial x_2} h - \rho \frac{\partial h}{\partial x_2} \right) - dh \right] x_1 dx_1 dx_2 = 0 \quad (11)$$

For the approximate problem (and the exact problem), ρ is required to be continuous throughout the problem domain, but derivatives may or may not be continuous across element boundaries. The above equation then requires the term dh to be equal to terms which collectively can be discontinuous across element boundaries. Now, the previous numerical results and the physical nature of the problem both indicate that the solution to the exact problem should yield a smooth function (continuous with continuous derivatives) for the acoustic density ρ . However, the final form of the approximate problem, resulting from integration by parts to form the weak problem, does not force continuity of derivatives of ρ across element boundaries. Thus, numerical error in approximating the exact solution ρ can produce an approximate solution which has discontinuous derivatives at the element boundaries. Requiring d to be continuous across element boundaries may result in a solution for d which attempts to approximate the terms which are discontinuous due to approximation error. This preceding argument is obviously not a rigorous error analysis of the approximate problem; however, it *does suggest modifying the weak problem to allow d to be discontinuous in both the x_1 and x_2 directions.* Thus, the approximate solution space

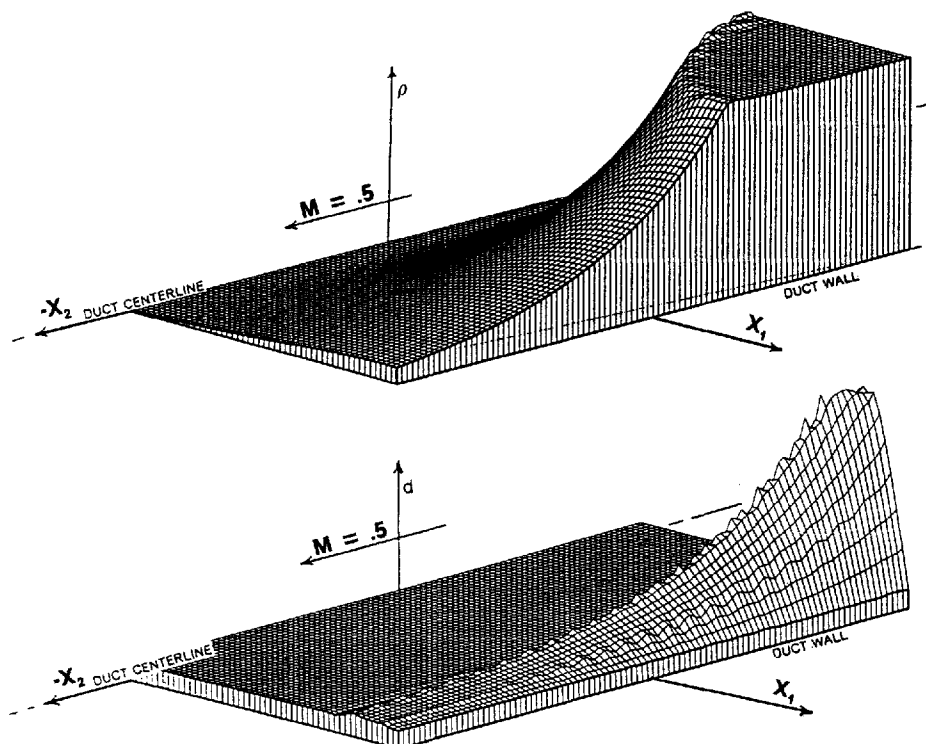


Figure 8. Same case as Figure 6, with eight elements across the region of sheared flow and a biquadratic approximation for d

D_h is replaced by a space D_h^\times which will be defined to be the set of all *bilinear* finite element approximate functions which may be (but are not required to be) discontinuous at element boundaries. This approximate equation will generally produce a non-square matrix problem to be solved. This is due to the asymmetry in the approximation spaces for d and g ; that is, d belongs to the set D_h^\times , the class of functions which may be discontinuous in all directions, but g belongs to the set G_h , the class of functions which are continuous in the axial direction. This rectangular system of algebraic equations, if carefully posed, can be solved by a least-squares method. As an alternative to using a least-squares method, the problem can be solved for all g belonging to D_h^\times instead of G_h . This produces a square matrix which can be solved by standard 'frontal' techniques.¹² It can be shown that if a solution to this alternate square matrix problem exists, then it is also a solution to the problem which produced the rectangular matrix. A solution to this symmetrical (square matrix) approximate problem ($d \in D_h^\times$, $g \in D_h^\times$) for the cut-off mode launch case is shown in Figure 9. The finite element mesh used is the unrefined mesh of 21 elements axially and 12 elements radially, with four elements across the sheared flow, and the function d is approximated on each element by the less accurate *bilinear* polynomials. It is apparent that this modified approximate problem gives a smooth solution for the mode-launching check cases, using fewer degrees of freedom, but it is accomplished in a somewhat less straightforward manner.

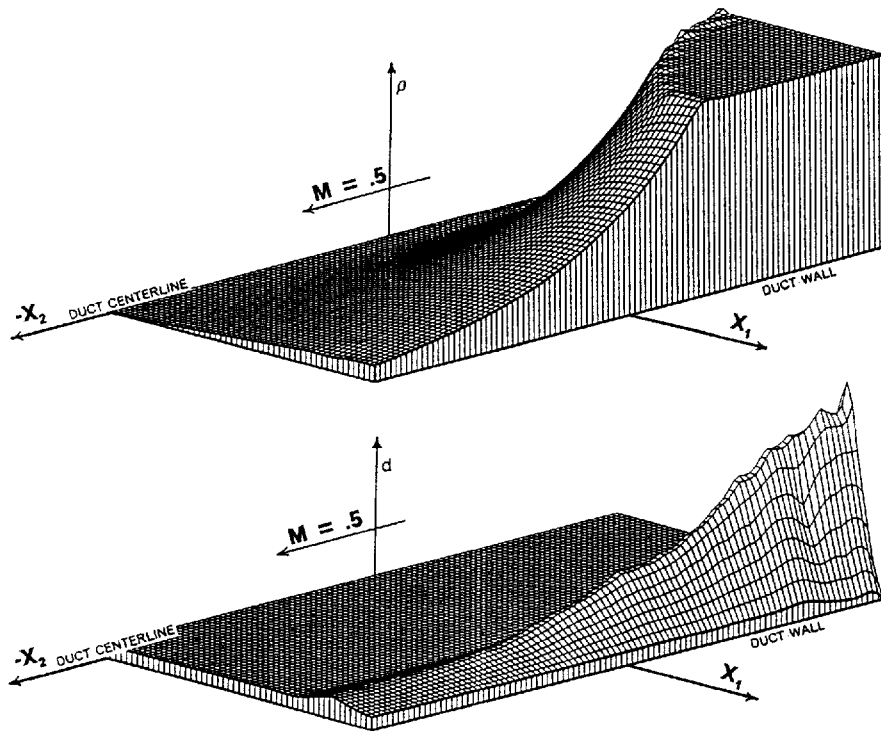


Figure 9. Same case as Figure 6, but using the modified numerical method allowing d to be discontinuous at the element boundaries, with four elements across the region of sheared flow and a bilinear approximation for d

PROPELLER RESULTS

Finally, we are prepared to solve the forced duct problem for a typical propeller distribution. Acoustic sources representing a two bladed propeller are placed in a duct containing uniform flow of $M=0.5$ Mach number (no shear) with $\hat{k}_n=4.0$ (having one cut-on mode). The propeller model is a Guten-type which represents the propeller by rotating acoustic sources and doublets.^{5,6} The solution method uses the *new* formulation with symmetrical function spaces, d and g both belonging to D_h^x for the approximate problem. The acoustic density ρ is approximated on an element by biquadratic polynomials, and d is approximated by bilinear polynomials with discontinuities allowed across element boundaries. These results are presented in Figures 10 and 11 for the fundamental mode, $m=2$. This same problem is solved for a sheared flow in the form of a linear boundary layer profile in the outer 20% of the duct ($M=0.5$ at $x_1=0.8$, varying linearly to $M=0$ at the wall). These results are presented in Figures 12 and 13. It can be seen that the major effect of the sheared flow is to reduce the acoustic pressure significantly in the area upstream of the propeller, while having little effect on the acoustic pressure downstream. This is in accord with the expectation that the slower flow near the wall should refract upstream-travelling waves away from the wall, and should refract downstream-travelling waves toward the wall.

Then this solution is compared with the results calculated using a different method developed by Eversman² to solve the sheared flow acoustic problem in a duct. This method involves

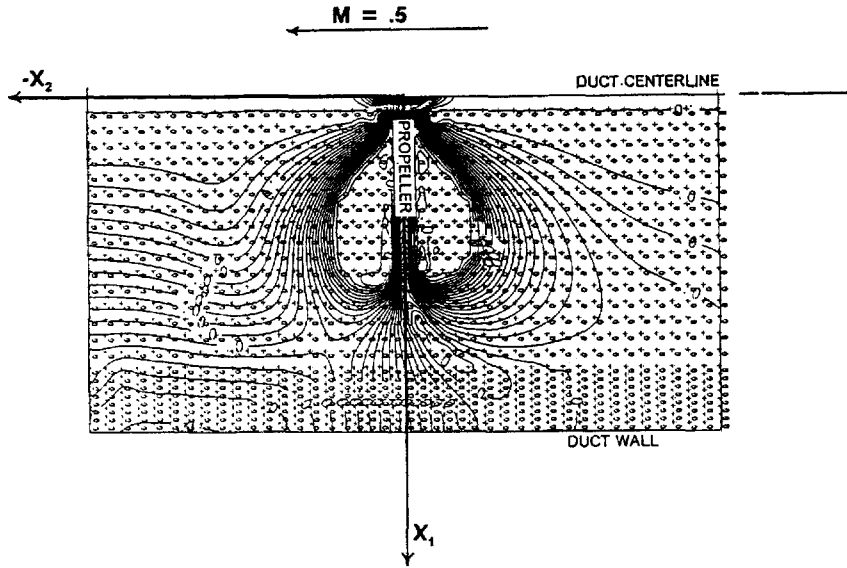


Figure 10. Acoustic density amplitude lines for the fundamental tone of a two-bladed propeller extending to half the duct radius, with uniform flow and one duct mode cut-on

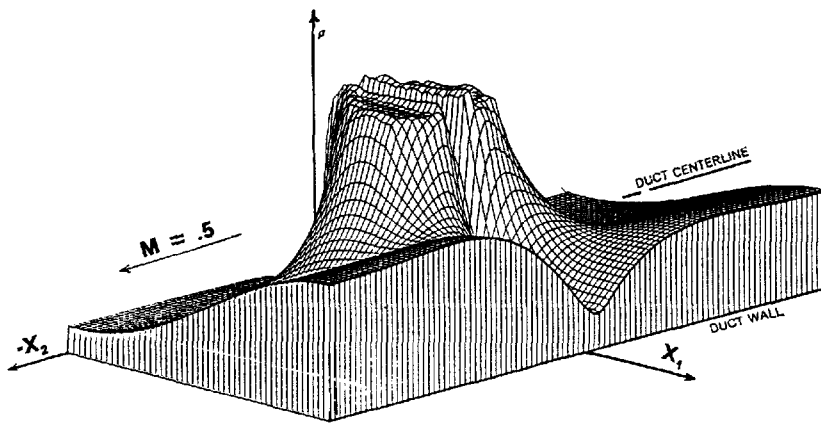


Figure 11. Acoustic density amplitude as a function of position in the duct for the fundamental tone of a two-bladed propeller extending to half the duct radius, with uniform flow and one duct mode cut-on

dividing the region containing sheared flow into annular regions in which the flow Mach number can be assumed to be constant. Mach number can vary from region to region in the radial direction to approximate the sheared flow profile. In the limit, as the number of annular divisions becomes large, this stepwise approximation of the flow profile approaches the continuous profile. Since the Mach number is constant in each region, the second-order acoustic wave equation for non-sheared flow holds on the interior of the region. This equation is readily solved on each annular region using an existing finite element method for the second-order equation. The physics

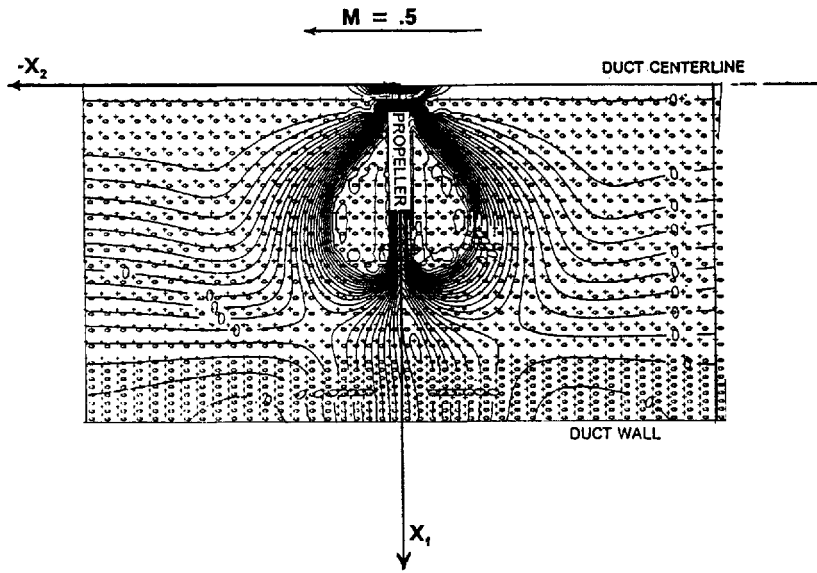


Figure 12. Acoustic density amplitude lines for the fundamental tone of a two-bladed propeller extending to half the duct radius, with sheared flow near the duct wall and one duct mode cut-on

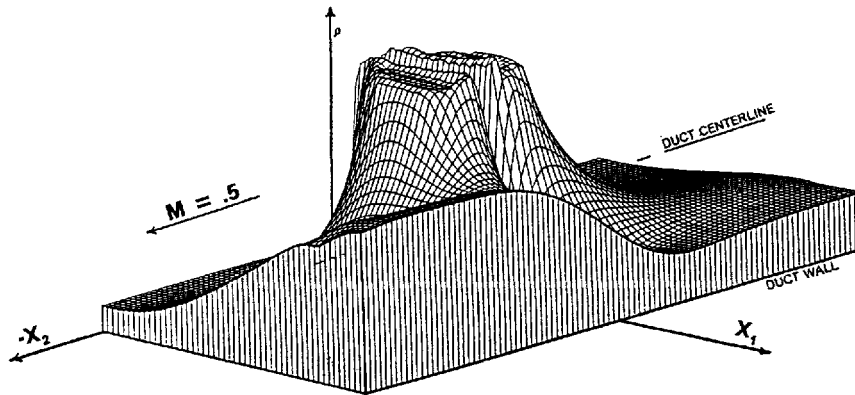


Figure 13. Acoustic density amplitude as a function of position in the duct for the fundamental tone of a two-bladed propeller extending to half the duct radius, with sheared flow near the duct wall and one duct mode cut-on

of the situation gives boundary conditions in terms of the jump in Mach number across the annular region interfaces. These boundary conditions result from the requirement of continuity of particle displacement across the boundary between regions of different Mach numbers. Using this method to solve the identical propeller acoustic problem above gives the results shown in Figures 14 and 15. This solution was calculated using biquadratic quadrilateral elements to approximate acoustic pressure, with the same finite element mesh of 21 elements axially and 12 elements radially. The propeller model used was slightly different from that used in a previous publication

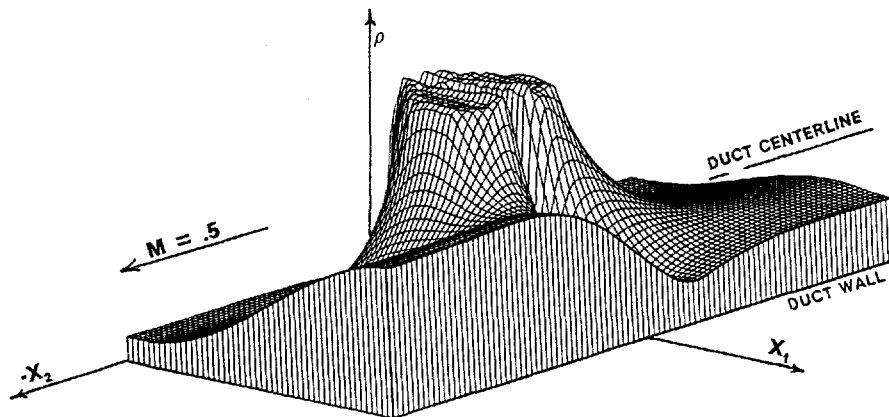


Figure 14. Results from stepwise approximation of sheared flow, showing acoustic density amplitude lines for the fundamental tone of a two-bladed propeller extending to half the duct radius, with sheared flow near the duct wall and one duct mode cut-on

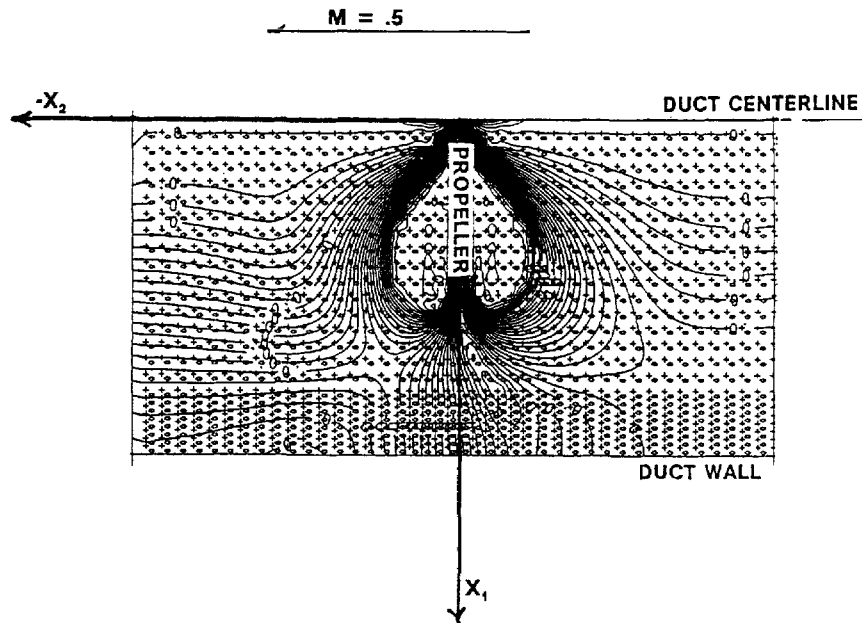


Figure 15. Results from stepwise approximation of sheared flow, showing acoustic density amplitude as a function of position in the duct for the fundamental tone of a two-bladed propeller extending to half the duct radius, with sheared flow near the duct wall and one duct mode cut-on

of the authors. The agreement between these results and the previous solution using the methods of this paper validate both the numerical methods for solving the acoustic field of a propeller in sheared flow in a circular duct.

CONCLUSIONS

The main advantage of the finite element formulation presented here for solving the third-order convected acoustic wave equation for sheared flow is that it is an extension of a successful

formulation of the second-order equation for unsheared flow. Decomposing the third-order sheared flow equation into a second-order and a first-order equation, choosing nine-noded biquadratic elements with continuity across the domain to approximate the acoustic density (the same elements used with unsheared flow) and choosing four-noded discontinuous bilinear elements to approximate the sheared flow artificial variable gives a finite element formulation similar to that used for unsheared flow. This allows the application of the extensive prior experience and knowledge of the type and number of elements required to represent accurately the acoustic density, or pressure, in convected flow situations. The numerical method is validated by numerous numerical experiments and by comparison with an alternate formulation which relies on a piecewise constant representation of the flow velocity profile to reduce the problem to second order. While a mathematical verification of the weak and approximate problems is desirable, the numerical validation is sufficient to demonstrate the validity of the formulation. A rigorous mathematical analysis is left for future work.

REFERENCES

1. W. Eversman and K. J. Baumeister, 'Modeling of wind tunnel wall effects on the radiation characteristics of acoustic sources', *AIAA Paper 84-2364*, October 1984.
2. W. Eversman, 'The effect of the wind tunnel wall boundary layer on the acoustic testing of propellers', AIAA Aeroacoustics Conference, San Antonio, TX, April 1989.
3. K. J. Baumeister and W. Eversman, 'Modeling of wind tunnel wall absorption on the acoustic radiation characteristics of propellers', *AIAA Paper 86-1876*, July 1986.
4. W. Mohring, 'Über Schallwellen in Scherströmungen', *Fortschritte der Akustik, DAGA 76*, VDI, Dusseldorf, 1976, pp. 543–546.
5. W. Eversman and J. E. Steck, 'Finite element modelling of acoustic singularities with application to near and far field propeller noise', *J. Aircraft*, **23**(4), 275–282 (1986).
6. L. J. Gutin, 'On the sound field of a rotating propeller', *NACA TM 1195*, 1948.
7. E. B. Becker, G. F. Carey and J. T. Oden, *Finite Elements—An Introduction, Vol. I*, Prentice-Hall, Englewood Cliffs, NJ, 1981.
8. J. T. Oden and J. N. Reddy, *An Introduction to the Mathematical Theory of Finite Elements*, Wiley, New York, 1976, pp. 89–144.
9. P. M. Morse, *Vibration and Sound*, McGraw-Hill, New York, 1948.
10. P. M. Morse and U. Ingard, *Theoretical Acoustics*, McGraw-Hill, New York, 1968.
11. R. J. Astley and W. Eversman, 'A finite element formulation of the eigenvalue problem in lined ducts with flow', *J. Sound Vib.*, **65**(1), 61–74 (1979).
12. B. M. Irons, 'A frontal solution program for finite element analysis', *Int. j. numer. methods eng.*, **2**, 5–32 (1970).
13. R. J. Astley and W. Eversman, 'Acoustic transmission in non-uniform ducts with mean flow. Part II. The finite element method', *J. Sound Vib.*, **74**(1), 103–121 (1981).
14. J. W. S. Rayleigh, *The Theory of Sound*, Dover, New York, 1945.